EUROPEAN JOURNAL OF PURE AND APPLIED MATHEMATICS
Vol. 13, No. 4, 2020, 766-778
ISSN 1307-5543 – www.ejpam.com
Published by New York Business Global

Free vibration analysis of thick FGM spherical shells based on a third-order shear deformation theory

Mohammad Zannon[1,*],Abdullah Abu-Rqayiq[2],Ammar Al-bdour[1]

[1] *Department of Mathematics, Tafila Technical University, Tafila, Jordan*
[2] *Department of Mathematics and Statistics, Texas AM University , Corpus Christi, USA*

Abstract. In this paper, we consider problems associated with free vibration of functionally graded thick spherical shells. We perform our analysis by collecting the radial basis functions, according to the third-order shear deformation theory that accounts the thickness deformation consuming the principle of virtual work. Numerical results which include spherical shell panels with all edges simply supported or clamped are presented to validate the accuracy of the present approach.

2020 Mathematics Subject Classifications: 74H15, 74H45, 74S30
Key Words and Phrases: Free vibration, Spherical shells, functionally graded materials, radial basis functions

1. Introduction

Functionally graded materials (FGM) have enormous application potential in modern technology such as aerospace. The use of FGM provides means to solve the problem of high transverse shear stresses, which are induced when two similar materials with different properties are bonded. The material properties are varied over the thickness of the bond by mixing the different materials. FGM can minimize the thermal stress concentration produced by the high temperature gradient. The vibration of the response of FGM beams has been studied in different ways, including analytical studies, numerical approaches, and the finite element method. The latter method is the most common numerical procedure for the analysis of the shells. Continuous development has resulted in complex structural designs of the materials; we therefore require a careful analysis in addition to the numerical methods to solve the mathematical shell models of these complex structures. Spherical shells are used in many applications, for example, in circular forms such as the nose of a plane or the caps of pressurized cylindrical tanks. The geometrical property of functionally graded (FG) spherical shells also leads to applications such as various

*Corresponding author.
DOI: https://doi.org/10.29020/nybg.ejpam.v13i4.3826

Email addresses: zanno1ms@gmail.com (M. Zannon),
Abdullah.aburqayiq@tamucc.edu (A. Abu-Rqayiq), ammarbdoor@gmail.com (A. Al-bdour)

reservoirs, interstage and spherical caps [10],[12]. Tomabene and Viola [21] carried out several studies on vibration solutions for FG spherical shell structures by applying the GDQ method. Considering the stretching and predominantly flexural vibration, Reddy and Cheng [17] discussed the properties of FG spherical, shallow shells by applying the classical theory and the first-order and third-order shear deformation theories. In the structure of the higher-order shear deformation theory (HSDT), Neves et al. [12] investigated the free vibration behaviours of FG shell structures, in which the expressions of motion and the boundary restraints were acquired by Carreras unified formulation. Kar and Panda [10] analyzed the vibration characteristics of the FG spherical shell structure based on the HSDT, and the analytical model is discretised by using quadrilateral Lagrangian element [1],[11] Meshfree techniques are often used to solve this problem. One such method is the radial base function (RBF) collocation method [2],[6],[13]. The use of radial basis function for the analysis of structures and materials has been previously studied [1],[7],[8],[9],[10],[11],[12],[13],[14],[15],[16],[17],[18]. Brischetto and Carrera (2010) applied the unified formulation (UF) in several finite element analyses of shells by using the Riessners mixed vibrational theorem or by using the principle of virtual Displacements. UF can help obtain the external force terms, the stiffness matrix components, and the inertia terms. An approach proposed by [20],[27],[28] was employed in this work which uses a third-order shear deformation theory (TSDT), allowing for through the thickness deformations . We also study the impact of $\varepsilon_{zz} \neq 0$ in these problems. The numerical examples given in this study demonstrate how effective the current approach is in predicting the free vibrations of thick spherical FG shells. The advantage of the current technique in expecting free vibrations of thick FG spherical shells are established thru numerical examples.The accuracy and reliability of the present method are verified by comparing our results to other available numerical results in literature [20].

2. Theoretical Formulation

2.1. Functionally Grade Material properties

FGM is formed by a mixture of ceramic and metal as shown in Figure 1. The material properties change continuously from one surface to the other according to a powerlaw of volume fraction [4],[15],[16]:

$$\begin{array}{l} P(z) = (P_c - P_m)\, V_c + P_m \\ V_c(z) = \left(\frac{1}{2} + \frac{z}{h}\right)^n \end{array} \tag{1}$$

where $P(z)$ represents the effective material properties: Young's modulus E, density ρ and Poisson ratio v ; P_c and P_m denote the properties of the Aluminum and Alumina, respectively; $V_c(z)$ is the volume fractions of the Aluminum; h the thickness of structure; is the $z \in \left[\frac{-h}{2}, \frac{h}{2}\right]$ the volume fraction exponent and $n \geq 0$ thickness coordinate of the structure.

2.2. Formulation

The shell structure is typically used in a typical vehicle's outer body. Some of these shell structures are flat, but most of them are curved in nature, so they are called shells [28],[29]. Plates are a special type of shells, so the focus in modelling and analyses has been on shells. Shells bodies are in three dimensions, one of which is thickness, which is small compared to the other two dimensions. Shell structure theories are based upon the three-dimensional (3D) theory of elasticity, which is costly and time-consuming. A schematic diagram of this geometry is shown in Figure 2.
On the basis of the Third-order shear deformation shell theory and applying the displacement field [29] we have

$$\begin{aligned} u(\alpha,\beta,z) &= u_0(\alpha,\beta) + z\psi_\alpha(\alpha,\beta) + z^3\varphi_\alpha(\alpha,\beta) \\ v(\alpha,\beta,z) &= v_0(\alpha,\beta) + z\psi_\beta(\alpha,\beta) + z^3\varphi_\beta(\alpha,\beta) \\ w(\alpha,\beta,z) &= w_0(\alpha,\beta) + z\psi_z(\alpha,\beta) \end{aligned} \tag{2}$$

where $\frac{-h}{2} \le z \le \frac{h}{2}$, h is the shell thickness, u_0, v_0 and w_0 are middle surface displacements of the shell, ψ_α, ψ_β, ψ_z are middle surface rotations and $\varphi_\alpha, \varphi_\beta$ are higher order terms rotation of transverse normal. Here, we use the method as the basis for a free vibration study of FG spherical shells [1],[11],[12],[22].
The fundamental nucleo $k_{uu}^{\kappa\tau s}$ is reported for functionally graded doubly curved spherical shells (radii of curvature in both α and β directions (see Fig. 2) [1],[5],[6],[7]:

$$\begin{aligned} \left(\mathbf{K}_{uu}^{\tau sk}\right)_{11} = &-\frac{E^\kappa\left(1-(v^\kappa)^2\right)}{1-3(v^\kappa)^2-2(v^\kappa)^3} J_{\beta/\alpha}^{k\tau s}\partial_\alpha^s\partial_\alpha^\tau - \frac{E^\kappa}{2(1+v^\kappa)} J_{\alpha/\beta}^{k\tau s}\partial_\beta^s\partial_\beta^\tau \\ &+\frac{E^\kappa}{2(1+v^\kappa)}\left(J_{\alpha\beta}^{k\tau_Z s_z} - \frac{1}{\mathrm{R}} J_\beta^{k\tau_z s} - \frac{1}{R} J_\beta^{k\tau s_z} + \frac{1}{R^2} J_{\beta/\alpha}^{k\tau s}\right) \end{aligned} \tag{3}$$

$$\left(\mathbf{K}_{uu}^{\tau Sk}\right)_{12} = -\frac{E^\kappa\left(v^\kappa+(v^\kappa)^2\right)}{1-3(v^\kappa)^2-2(v^\kappa)^3} J^{k\tau s}\partial_\alpha^\tau\partial_\beta^s - \frac{E^\kappa}{2(1+v^\kappa)} J^{k\tau s}\partial_\alpha^s\partial_\beta^\tau \tag{4}$$

$$\begin{aligned} \left(\mathbf{K}_{uu}^{\tau sk}\right)_{13} = &-\frac{E^\kappa\left(1-(v^\kappa)^2\right)}{1-3(v^\kappa)^2-2(v^\kappa)^3}\frac{1}{\mathrm{R}} J_{\beta/\alpha}^{k\tau s}\partial_\alpha^\tau - \frac{E^\kappa\left(v^\kappa+(v^\kappa)^2\right)}{1-3(v^\kappa)^2-2(v^\kappa)^3}\frac{1}{\mathrm{R}} J_{\alpha\alpha}^{k\tau s}\partial_\alpha^\tau \\ &-\frac{E^\kappa\left(v^\kappa+(v^\kappa)^2\right)}{1-3(v^\kappa)^2-2(v^\kappa)^3} J_\beta^{k\tau_S}\partial_\alpha^\tau + \frac{E^\kappa}{2(1+v^\kappa)}\left(J_\beta^{k\tau_z s}\partial_\alpha^s - \frac{1}{\mathrm{R}} J_{\beta/\alpha}^{\mathrm{k}\tau S}\partial_\alpha^s\right) \end{aligned} \tag{5}$$

$$\left(\mathbf{K}_{uu}^{\tau sk}\right)_{21} = -\frac{E^\kappa\left(v^\kappa+(v^\kappa)^2\right)}{1-3(v^\kappa)^2-2(v^\kappa)^3} J^{k\tau s}\partial_\alpha^s\partial_\beta^\tau - \frac{E^\kappa}{2(1+v^\kappa)} J^{k\tau s}\partial_\alpha^\tau\partial_\beta^s \tag{6}$$

$$\left(\mathbf{K}_{uu}^{\tau sk}\right)_{22} = -\frac{E^\kappa}{2(1+v^\kappa)} J_{\beta/\alpha}^{k\tau s}\partial_\alpha^S\partial_\alpha^\tau + \frac{E^\kappa}{2(1+v^\kappa)}\left(U_{\alpha\beta}^{k\tau_Z S_z} - \frac{1}{\mathrm{R}} J_\alpha^{k\tau_Z S} - \frac{1}{\mathrm{R}} J_\alpha^{k\tau s_Z} + \frac{1}{R^2} J_{\alpha/\beta}^{k\tau S}\right) \tag{7}$$

$$\begin{aligned}\left(\mathbf{K}_{uu}^{\tau sk}\right)_{23} &= -\frac{E^{\kappa}\left(v^{\kappa}+(v^{\kappa})^{2}\right)}{1-3(v^{\kappa})^{2}-2(v^{\kappa})^{3}}\frac{1}{\mathrm{R}}J_{\beta\beta}^{k\tau s}\partial_{\beta}^{\tau}-\frac{E^{\kappa}\left(v^{\kappa}+(v^{\kappa})^{2}\right)}{1-3(v^{\kappa})^{2}-2(v^{\kappa})^{3}}J_{\alpha}^{k\tau_{S}}\partial_{\beta}^{\tau}\\ &+\frac{E^{\kappa}}{2(1+v^{\kappa})}\left(J_{\alpha}^{k\tau_{Z}s}\partial_{\beta}^{s}-\frac{1}{\mathrm{R}}J_{\alpha/\beta}^{k\tau s}\partial_{\beta}^{s}\right)\end{aligned} \tag{8}$$

$$\begin{aligned}\left(\mathbf{K}_{uu}^{\tau sk}\right)_{31} &= \frac{E^{\kappa}\left(1-(v^{\kappa})^{2}\right)}{1-3(v^{\kappa})^{2}-2(v^{\kappa})^{3}}\frac{1}{\mathrm{R}}J_{\beta/\alpha}^{k\tau}\partial_{\alpha}^{s}+\frac{E^{\kappa}\left(v^{\kappa}+(v^{\kappa})^{2}\right)}{1-3(v^{\kappa})^{2}-2(v^{\kappa})^{3}}\frac{1}{\mathrm{R}}J_{\alpha}^{k\tau}\partial_{\alpha}^{s}\\ &+\frac{E^{\kappa}\left(v^{\kappa}+(v^{\kappa})^{2}\right)}{1-3(v^{\kappa})^{2}-2(v^{\kappa})^{3}}J_{\beta}^{k\tau_{Z}s}\delta_{\alpha}^{s}-\frac{E^{\kappa}}{2(1+v^{\kappa})}\left(J_{\beta}^{k\tau s_{Z}}\partial_{\alpha}^{\tau}-\frac{1}{\mathrm{R}}J_{\beta/\alpha}^{k\tau S}\partial_{\alpha}^{\tau}\right)\end{aligned} \tag{9}$$

$$\begin{aligned}(\mathbf{K}_{uu}^{\tau_{Sk}})_{32} &= \frac{E^{\kappa}\left(v^{\kappa}+(v^{\kappa})^{2}\right)}{1-3(v^{\kappa})^{2}-2(v^{\kappa})^{3}}\frac{1}{\mathrm{R}}J_{\beta k}^{k\tau s}\partial_{\beta}^{s}+\frac{E^{\kappa}\left(v^{\kappa}+(v^{\kappa})^{2}\right)}{1-3(v^{\kappa})^{2}-2(v^{\kappa})^{3}}J_{\alpha}^{k\tau_{z}s}\partial_{\beta}^{s}\\ &-\frac{E^{\kappa}}{2(1+v^{\kappa})}\left(J_{\alpha}^{k\tau s_{z}}\partial_{\beta}^{\tau}-\frac{1}{\mathrm{R}}J_{\alpha/\beta}^{k\tau s}\partial_{\beta}^{\tau}\right)\end{aligned} \tag{10}$$

$$\begin{aligned}\left(\mathbf{K}_{uu}^{\tau sk}\right)_{33} &= \frac{E^{\kappa}\left(1-(v^{\kappa})^{2}\right)}{1-3(v^{\kappa})^{2}-2(v^{\kappa})^{3}}\frac{1}{R^{2}}J_{\beta/\alpha}^{k\tau S}+\frac{E^{\kappa}\left(1-(v^{\kappa})^{2}\right)}{1-3(v^{\kappa})^{2}-2(v^{\kappa})^{3}}3_{\alpha\beta}^{k\tau_{\tau}S_{z}}\\ &+2\frac{E^{\kappa}\left(v^{\kappa}+(v^{\kappa})^{2}\right)}{1-3(v^{\kappa})^{2}-2(v^{\kappa})^{3}}\frac{1}{\mathrm{R}}J_{1}^{k\tau s}+\frac{E^{\kappa}\left(v^{\kappa}+(v^{\kappa})^{2}\right)}{1-3(v^{\kappa})^{2}-2(v^{\kappa})^{3}}\frac{1}{R}\left(J_{\beta}^{k\tau_{z}s}+J_{\beta}^{k\tau s_{z}}\right)\\ &+\frac{E^{\kappa}\left(v^{\kappa}+(v^{\kappa})^{2}\right)}{1-3(v^{x})^{2}-2(v^{x})^{3}}\frac{1}{\mathrm{R}}\left(\mathrm{U}_{\alpha}^{k\tau_{z}s}+J_{\alpha}^{k\tau_{z}}\right)-\frac{E^{\kappa}}{2(1+v^{\kappa})}J_{\alpha/\beta}^{k\tau s}\partial_{\beta}^{s}\partial_{\beta}^{\tau}\\ &-\frac{E^{\kappa}}{2(1+v^{\kappa})}J_{\beta/\alpha}^{k\tau s}\partial_{\alpha}^{s}\alpha_{\alpha}^{\tau}\end{aligned} \tag{11}$$

where

$$\left(J^{k\tau S},J_{\alpha}^{k\tau S},J_{\beta}^{k\tau S},J_{\frac{\alpha}{\beta}}^{k\tau s},J_{\frac{\beta}{\alpha}}^{k\tau s},,J_{\alpha\beta}^{k\tau S}\right)=\int_{A_{k}}F_{\tau}F_{S}\left(1,1+\frac{z}{R},1+\frac{z}{R},1,1,1\right)dz \tag{12}$$

$$\left(J^{k\tau_{Z}s},J_{\alpha}^{k\tau_{Z}S},J_{\beta}^{k\tau_{Z}s},J_{\frac{\alpha}{\beta}}^{k\tau_{Z}S},J_{\frac{\beta}{\alpha}}^{k\tau_{Z}S},J_{\alpha\beta}^{k\tau_{Z}S}\right)=\int_{A_{k}}\frac{\partial F_{\tau}}{\partial z}F_{S}\left(1,1+\frac{z}{R},1+\frac{z}{R},1,1,1\right)dz \tag{13}$$

$$\left(J^{k\tau S_{Z}},J_{\alpha}^{k\tau S_{Z}},J_{\beta}^{k\tau S_{Z}},J_{\frac{\alpha}{\beta}}^{k\tau S_{Z}},J_{\frac{\beta}{\alpha}}^{k\tau S_{Z}},J_{\alpha\beta}^{k\tau S_{Z}}\right)=\int_{A_{k}}F_{\tau}\frac{\partial F_{S}}{\partial z}\left(1,1+\frac{z}{R},1+\frac{z}{R},1,1,1\right)dz \tag{14}$$

$$\left(J^{k\tau_2 s_2}, J^{k\tau_2 S_z}_{\alpha}, J^{k\tau_2 s_z}_{\beta}, J^{k\tau_z s_z}_{\frac{\alpha}{\beta}}, J^{k\tau_z s_z}_{\beta}, J^{k\tau_z s_z}_{\alpha\beta}\right) = \int_{A_k} \frac{\partial F_\tau}{\partial z}\frac{\partial F_s}{\partial z}\left(1, 1+\frac{z}{R}, 1+\frac{z}{R}, 1, 1, 1\right) dz \tag{15}$$

The application of boundary conditions makes use of the fundamental nucleo Π_d in the form [13],[14],[15],[17]:

$$(\Pi^{\tau_{SK}}_{uu})_{11} = \cos(\varphi_\alpha)\frac{E^\kappa\left(1-(v^\kappa)^2\right)}{1-3(v^\kappa)^2-2(v^\kappa)^3} J^{k\tau S}_{\beta/\alpha}\partial^S_\alpha + \cos(\varphi_\beta)\frac{E^\kappa}{2(1+v^\kappa)} J^{k\tau}_{\alpha/\beta}\partial^S_\beta \tag{16}$$

$$\left(\Pi^{\tau Sk}_{uu}\right)_{12} = \cos(\varphi_\alpha)\frac{E^\kappa\left(\nu^\kappa+(\nu^\kappa)^2\right)}{1-3(\nu^\kappa)^2-2(\nu^\kappa)^3} J^{k\tau s}\partial^S_\beta + \cos(\varphi_\beta)\frac{E^\kappa}{2(1+\nu^\kappa)} J^{k\tau s}\partial^S_\alpha \tag{17}$$

$$\begin{aligned}\left(\Pi^{\tau sk}_{uu}\right)_{13} = {} & \cos(\varphi_\alpha)\tfrac{1}{\mathrm{R}}\frac{E^\kappa\left(1-(v^\kappa)^2\right)}{1-3(v^\kappa)^2-2(v^\kappa)^3} J^{k\tau S}_{\beta/\alpha} + \cos(\varphi_\alpha)\tfrac{1}{\mathrm{R}}\frac{E^\kappa\left(v^\kappa+(v^\kappa)^2\right)}{1-3(v^\kappa)^2-2(v^\kappa)^3} J^{k\tau s} \\ & + \cos(\varphi_\alpha)\frac{E^\kappa\left(\nu^\kappa+(\nu^\kappa)^2\right)}{1-3(\nu^\kappa)^2-2(\nu^\kappa)^3} J^{k\tau_2}_{\beta}\end{aligned} \tag{18}$$

$$\left(\Pi^{\tau sk}_{uu}\right)_{21} = \cos(\varphi_\beta)\frac{E^\kappa\left(\nu^\kappa+\left(\nu^K\right)^2\right)}{1-3(\nu^\kappa)^2-2(\nu^\kappa)^3} J^{k\tau s}\partial^S_\alpha + \cos(\varphi_\alpha)\frac{E^\kappa}{2(1+\nu^\kappa)} J^{k\tau S}\delta^S_\beta \tag{19}$$

$$(\Pi^{\tau_{SK}}_{uu})_{22} = \cos(\varphi_\alpha)\frac{E^\kappa}{2(1+v^\kappa)} J^{k\tau S}_{\beta/\alpha}\partial^S_\alpha \tag{20}$$

$$\left(\Pi^{\tau Sk}_{uu}\right)_{23} = \cos(\varphi_\beta)\frac{1}{\mathrm{R}}\frac{E^\kappa\left(v^\kappa+(v^\kappa)^2\right)}{1-3(v^\kappa)^2-2(v^\kappa)^3} J^{kts} + \cos(\varphi_\beta)\frac{E^\kappa\left(v^\kappa+(v^\kappa)^2\right)}{1-3(v^\kappa)^2-2(v^\kappa)^3} J^{k\tau_\varepsilon z_z}_{\alpha} \tag{21}$$

$$\left(\Pi^{\tau sk}_{uu}\right)_{31} = -\cos(\varphi_\alpha)\frac{1}{\mathrm{R}}\frac{E^\kappa}{2(1+v^\kappa)} J^{k\tau s}_{\beta/\alpha} + \cos(\varphi_\alpha)\frac{E^\kappa}{2(1+v^\kappa)} J^{k\tau s_z}_{\beta} \tag{22}$$

$$\left(\Pi^{\tau sk}_{uu}\right)_{32} = -\cos(\varphi_\beta)\frac{1}{\mathrm{R}}\frac{E^\kappa}{2(1+v^\kappa)} J^{k\tau s}_{\alpha/\beta} + \cos(\varphi_\beta)\frac{E^\kappa}{2(1+v^\kappa)} J^{k\tau s_z}_{\alpha} \tag{23}$$

$$\left(\Pi^{\tau sk}_{uu}\right)_{33} = \cos(\varphi_\alpha)\frac{E^\kappa}{2(1+v^\kappa)} J^{k\tau s}_{\beta/\alpha}\partial^S_\alpha + \cos(\varphi_\beta)\frac{E^\kappa}{2(1+v^\kappa)} J^{k\tau S}_{\alpha/\beta}\partial^S_\beta \tag{24}$$

Different studies describe the radial base function $s(x)$ as a univariate continuous real-valued function that mainly depends on the distance between the origin or other fixed

center point [2],[9],[28].
Definition: [2],[9],[12] Let $\mathbb{R}^+ = \{x \in \mathbb{R}, x \geq 0\}$ be the non-negative half line and let $\phi : \mathbb{R}^+ \to \mathbb{R}$ be a continuous function with $\phi(0) \geq 0$ A radial basis function on $\mathbb{R}^d$ is a function of the form $\phi(\|x - x_i\|)$, where $x, x_i \in \mathbb{R}^d$ and $r = \|x - x_i\|$ denotes the Euclidean distance between x and x_i. If N points $\{x_i\}_{i=1}^N$ in $\mathbb{R}^d$ are chosen, then by custom $s(x) = \sum_{i=1}^N \lambda_i \phi(\|x - x_i\|); \lambda_i \in \mathbb{R}$ is called a radial basis functions as well.
The Euclidean distance is therefore real and non-negative and is a parameter for controlling the shape of the functions with effects on the convergence rate [1],[9],[12]. We consider the elliptic partial differential operator D acting in a bounded region Ω in $\mathbb{R}^n$, and $\partial\Omega$ is the boundary of the domain for purposes of the mathematical formulation.
Consider the following elliptic PDE problem presented in [2],[3],[8],[13],[23]:

$$Du(x) = f(x) \text{ in domain } \Omega$$

$$u(x) = g(x) \text{ in domain } \Omega$$

For scattered data $(x_i, u(x_i)) \in \mathbb{R}^{d+1}$ the approximation $s(x)$ for a real function $u(x)$ can be constructed by linear combinations of translations of one function $\phi(\|\cdot\|)$ of one variable which is centred at

$$\{x_i\}_{i=1}^N \subseteq \mathbb{R}^d, u(x) \approx s(x) = \sum_{i=1}^N \gamma_i \phi(\|x - x_i\|) \tag{25}$$

The most attractive feature of the RBF methods is that the location of centres can be chosen arbitrarily in the domain of interest. To determine the unknown coefficients $\gamma_i, i = 1, 2, 3, \ldots . N$, we impose the interpolation conditions on $s(x)$. This gives the $N \times N$ linear system

$$u(x_j) = \sum_{i=1}^N \gamma_i \phi(\|x_j - x_i\|) \tag{26}$$

where the γ_i's are unknown coefficients to be determined, N is the total number of nodes for which their N_L point are the interior points and ϕ is the radial basis function approximation of the function u [2],[11],[24]. Collocation with the PDE at the inner points and boundary conditions, there are the following observations at the boundary points:

$$\begin{cases} F(x_i) = Du(x_j) \approx \sum_{i=1}^N \gamma_i D\phi(\|x_j - x_i\|), \forall j = 1, 2, \ldots \ldots, N \\ G(x_i) = u(x_j) \approx \sum_{i=1}^N \gamma_i \phi(\|x_j - x_i\|), \forall j = N_{L+1}, \ldots \ldots \ldots, N \end{cases} \tag{27}$$

The coefficients $\{\gamma_j\}_{j=1}^N$ can be solved from the corresponding system of equations with the coefficient matrix structured as:

$$\begin{bmatrix} F \\ G \end{bmatrix} = \begin{bmatrix} D\phi \\ \phi \end{bmatrix} [\gamma] \tag{28}$$

For free vibration problems, a harmonic solution is assumed for the displacements and it is given in [2],[9],[24]. Substituting the harmonic expansion into equations (28), which can be written as an eigenvalue problem. Therefore, the resulting equations can be written in the following matrix form:

$$\{[D] - \lambda[\zeta]\}\{[\Delta]\} = 0 \tag{29}$$

where $\lambda = \omega^2$, ω is the natural frequency, $\{\Delta\}$ is the displacement vector and $\{\zeta\}$ collects all terms related to the inertial terms [26],[29].

2.3. Numerical Results

In this section, both theories (the third-order shear deformation theory and the radial base functions collocation for the free vibration study of functionally graded shell panels) are combined [1],[19],[20]. Examples below show spherical shell panels with all edges clamped or simply supported. Particular cases are also considered, namely isotropic materials (fully ceramic and metal) [24],[25],[26],[27],[28],[29]. Comparing the results with Pradyumna and Bandyopadhyay [11],[16] there is a marked improvement in HSDT and finite elements formulation. In the following example, consideration is given to the free vibration of simply supported and clamped FG spherical shell panels. The fundamental frequencies of a simply supported square and clamped FG spherical shell panels composed of aluminium and alumina, with the side-to-thickness ratio $a/h = 10$ are presented in tables 1, 2, 3, 4, 5 and 6 considering various side-to-radius ratios a/R as well as power-law exponent p. This technique possess similar properties as : Aluminumi:

$$E_m = 70GPa, v_m = 0.3, \rho_m = 270\text{Kg/m}^3$$

Alumina:

$$E_c = 380GPa, v_c = 0.3, \rho_c = 3000\text{Kg/m}^3$$

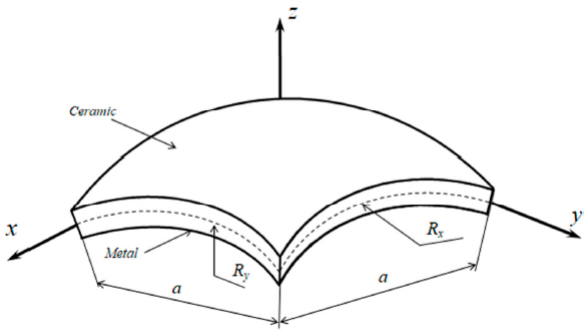

Figure 1: A functionally graded shell [15]

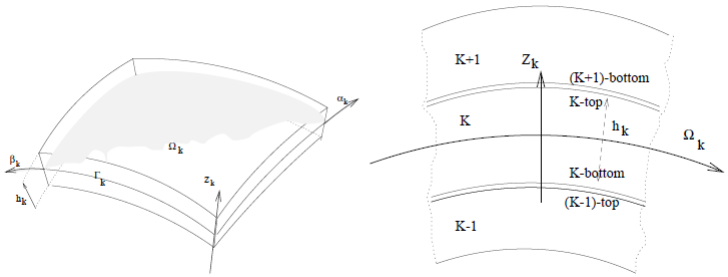

Figure 2: Geometry and notations for a multilayered shell [12]

Table 1: Fundamental frequencies of $CCCC$ square spherical shell panels collected of aluminum and alumina, $R/a = 0.5$ and $a/h = 10$, for various p

P	Ref [3]	Present $\varepsilon_{zz} \neq 0$	Ref [16]
0	173.9595	176.8240	176.8356
0.2	161.3704	162.2278	163.0460
0.5	147.4598	148.2765	149.0095
1	132.3396	133.1074	133.7710
2	116.4386	117.2276	117.9317
∞	80.7722	80.3306	79.8994

Table 2: Fundamental frequencies of $CCCC$ square spherical shell panels collected of aluminum and alumina, $R/a = 1$ and $a/h = 10$, for various p

P	Ref [3]	Present $\varepsilon_{zz} \neq 0$	Ref [16]
0	120.9210	122.2234	122.3533
0.2	112.2017	112.4581	112.8132
0.5	102.5983	102.8894	103.1490
1	92.2147	92.5215	92.6962
2	81.3963	81.7456	81.9179
∞	56.2999	55.7926	55.2827

Table 3: Fundamental frequencies of $CCCC$ square spherical shell panels collected of aluminum and alumina, $R/a = 5$ and $a/h = 10$, for various p

P	Ref [3]	Present $\varepsilon_{zz} \neq 0$	Ref [16]
0	73.5550	74.1879	75.2810
0.2	69.6597	68.9369	68.6329
0.5	64.6114	63.1508	62.0789
1	57.8619	56.3608	55.2302
2	37.3914	43.0285	49.0328
∞	33.2343	33.5202	34.0141

Table 4: Fundamental frequencies of $SSSS$ square spherical shell panels collected of aluminum and alumina, $R/a = 0.5$ and $a/h = 10$, for various p

P	Ref [3]	Present $\varepsilon_{zz} \neq 0$	Ref [16]
0	124.1581	125.2288	126.0882
0.2	115.7499	116.5276	117.0197
0.5	106.5014	107.2529	107.6572
1	96.2587	96.9763	97.2968
2	84.8206	85.5247	85.8028
∞	57.2005	7.1331	56.9702

Table 5: Fundamental frequencies of $SSSS$ square spherical shell panels collected of aluminum and alumina, $R/a = 1$ and $a/h = 10$, for various p

P	Ref [3]	Present $\varepsilon_{zz} \neq 0$	Ref [16]
0	44.0073	44.2264	44.4697
0.2	41.7782	41.0859	40.4211
0.5	38.7731	37.6092	36.4782
1	34.6009	33.4847	32.4101
2	28.7459	28.7646	28.8329
∞	19.8838	19.9828	20.0927

Table 6: Fundamental frequencies of $SSSS$ square spherical shell panels collected of aluminum and alumina, $R/a = 5$ and $a/h = 10$, for various p

P	Ref [3]	Present $\varepsilon_{zz} \neq 0$	Ref [16]
0	124.1581	125.2288	126.0882
0.2	115.7499	116.5276	117.0197
0.5	106.5014	107.2529	107.6572
1	96.2587	96.9763	97.2968
2	84.8206	85.5247	85.8028
∞	57.2005	7.1331	56.9702

3. Conclusions

Here we examine the previous work and continue to propose our own methods. Free vibration analyzes of FG spherical shells is examined. A third-order shear deformation theory that allows extensibility in the thickness direction was executed and the influence of $\varepsilon_{zz} \neq 0$ was studied. The main conclusion that can be drawn from this work is The fundamental frequency decreases as the ratio R/a increases, clamped FG shell panels present higher frequency values than simply supported ones and the fundamental frequency of FG spherical shell panels decreases as the exponent p in power-law increases. The effect of $\varepsilon_{zz} \neq 0$ shows significance in thicker shells and seems independent of the radius of curvature. The accuracy and reliability of the present method is carried out by comparing our present findings with those of available numerical results.

Acknowledgements

The authors thank the fund by the College of Science and Engineering at Texas A&M University-Corpus Christi.

References

[1] Yamna Belkhodja, Djamel Ouinas, Fatima Zohra Zaoui, and Hamida Fekirini. An exponential-trigonometric higher order shear deformation theory (hsdt) for bending, free vibration, and buckling analysis of functionally graded materials (fgms) plates. *Advanced Composites Letters*, 29:0963693519875739, 2020.

[2] Gurpreet Singh Bhatia and Geeta Arora. Radial basis function methods for solving partial differential equations-a review. *Indian Journal of Science and Technology*, 9(45):1–18, 2016.

[3] M Dottavio, D Ballhause, B Kröplin, and E Carrera. Closed-form solutions for the free-vibration problem of multilayered piezoelectric shells. *Computers & structures*, 84(22-23):1506–1518, 2006.

[4] AJM Ferreira. A formulation of the multiquadric radial basis function method for the analysis of laminated composite plates. *Composite structures*, 59(3):385–392, 2003.

[5] AJM Ferreira, E Carrera, M Cinefra, CMC Roque, and O Polit. Analysis of laminated shells by a sinusoidal shear deformation theory and radial basis functions collocation, accounting for through-the-thickness deformations. *Composites Part B: Engineering*, 42(5):1276–1284, 2011.

[6] AJM Ferreira and GE Fasshauer. Computation of natural frequencies of shear deformable beams and plates by an rbf-pseudospectral method. *Computer Methods in Applied Mechanics and Engineering*, 196(1-3):134–146, 2006.

[7] AJM Ferreira, CMC Roque, E Carrera, M Cinefra, and O Polit. Radial basis functions collocation and a unified formulation for bending, vibration and buckling analysis of laminated plates, according to a variation of murakamis zig-zag theory. *European Journal of Mechanics-A/Solids*, 30(4):559–570, 2011.

[8] AJM Ferreira, CMC Roque, and PALS Martins. Analysis of composite plates using higher-order shear deformation theory and a finite point formulation based on the multiquadric radial basis function method. *Composites Part B: Engineering*, 34(7):627–636, 2003.

[9] Ahmad Golbabai, Omid Nikan, and Jaber Ramezani Tousi. Note on using radial basis functions method for solving nonlinear integral equations. *Commun. Numer. Anal*, 81:2016, 2016.

[10] Vishesh Ranjan Kar and Subrata Kumar Panda. Free vibration responses of functionally graded spherical shell panels using finite element method. In *Gas Turbine India Conference*, volume 35161, page V001T05A014. American Society of Mechanical Engineers, 2013.

[11] DH Li, X Yang, RL Qian, and D Xu. Static and dynamic response analysis of functionally graded material plates with damage. *Mechanics of Advanced Materials and Structures*, 27(2):94–107, 2020.

[12] AMA Neves, AJM Ferreira, E Carrera, M Cinefra, CMC Roque, RMN Jorge, and CMM Soares. Free vibration analysis of functionally graded shells by a higher-order shear deformation theory and radial basis functions collocation, accounting for through-the-thickness deformations. *European Journal of Mechanics-A/Solids*, 37:24–34, 2013.

[13] AMA Neves, AJM Ferreira, E Carrera, CMC Roque, M Cinefra, RMN Jorge, and CMM Soares. Bending of fgm plates by a sinusoidal plate formulation and collocation with radial basis functions. *Mechanics Research Communications*, 38(5):368–371, 2011.

[14] T-K Nguyen, Karam Sab, and Guy Bonnet. Shear correction factors for functionally graded plates. *Mechanics of Advanced Materials and Structures*, 14(8):567–575, 2007.

[15] Tien Dat Pham, Quoc Hoa Pham, Van Duc Phan, Hoang Nam Nguyen, Van Thom Do, et al. Free vibration analysis of functionally graded shells using an edge-based smoothed finite element method. *Symmetry*, 11(5):684, 2019.

[16] S Pradyumna and JN Bandyopadhyay. Free vibration analysis of functionally graded curved panels using a higher-order finite element formulation. *Journal of Sound and Vibration*, 318(1-2):176–192, 2008.

[17] JN Reddy and Zhen-Qiang Cheng. Frequency correspondence between membranes and functionally graded spherical shallow shells of polygonal planform. *International journal of mechanical sciences*, 44(5):967–985, 2002.

[18] CMC Roque, AJM Ferreira, and RMN Jorge. Free vibration analysis of composite and sandwich plates by a trigonometric layerwise deformation theory and radial basis functions. *Journal of Sandwich Structures & Materials*, 8(6):497–515, 2006.

[19] Scott A Sarra. A numerical study of the accuracy and stability of symmetric and asymmetric rbf collocation methods for hyperbolic pdes. *Numerical Methods for Partial Differential Equations: An International Journal*, 24(2):670–686, 2008.

[20] Scott A Sarra. The matlab radial basis function toolbox. *Journal of Open Research Software*, 5(1), 2017.

[21] Erasmo Viola and Francesco Tornabene. Free vibrations of three parameter functionally graded parabolic panels of revolution. *Mechanics research communications*, 36(5):587–594, 2009.

[22] Song Xiang, Hong Shi, Ke-ming Wang, Yan-ting Ai, and Yun-dong Sha. Thin plate spline radial basis functions for vibration analysis of clamped laminated composite plates. *European Journal of Mechanics-A/Solids*, 29(5):844–850, 2010.

[23] J Yang and Hui-Shen Shen. Free vibration and parametric resonance of shear deformable functionally graded cylindrical panels. *Journal of Sound and Vibration*, 261(5):871–893, 2003.

[24] Suranon Yensiri and Ruth J Skulkhu. An investigation of radial basis function-finite difference (rbf-fd) method for numerical solution of elliptic partial differential equations. *Mathematics*, 5(4):54, 2017.

[25] M Zannon and M Qatu. Free vibration analysis of thick cylindrical composite shells using higher order shear deformation theory. *International Journal of Engineering Research and Management (IJERM)*, 1(7), 2014.

[26] M Zannon and M Qatu. Mathematical modeling of transverse shear deformation thick shell theory. *International Journal of Engineering Research and Management (IJERM)*, 1(7), 2014.

[27] Mohammad Zannon, Basma Al-Shutnawi, Hussam Alrabaiah, et al. Theories and analyses thick hyperbolic paraboloidal composite shells. *American Journal of Computational Mathematics*, 5(02):80, 2015.

[28] Mohammad Zannon and Hussam Alrabaiah. Mathematical formulation of laminated composite thick conical shells. *Journal of Mathematics Research*, 8(4), 2016.

[29] Mohammad Zannon et al. Fundamental frequency of laminated composite thick spherical shells. *Journal of Mathematics Research*, 11(1):57–63, 2019.